JOURNAL OF CATALYSIS **108**, 444–451 (1987)

Oxidation–Reduction Treatment of Rhodium Supported on Nonporous Silica Spheres

S. CHAKRABORTI,* A. K. DATYE,*[,1] AND N. J. LONG†[,2]

Department of Chemical & Nuclear Engineering, University of New Mexico, Albuquerque, New Mexico 87131, and †Center for Solid State Science, Arizona State University, Tempe, Arizona 85287

Received February 24, 1987; revised June 22, 1987

The structure of Rh crystallites subjected to oxidation–reduction treatment has been investigated by high-resolution transmission electron microscopy. The Rh was supported on 130-nm nonporous silica spheres so that the three-dimensional structure of the metal crystallites could be readily observed. After oxidation at 823 K and subsequent reduction at 473 K, the particles show images characterized by a lower contrast at the center. The edge-on views confirm that the particles are not toroidal but near spherical with a void at the center. This morphology is a result of the density difference between Rh metal and its oxide. The resulting metal crystallites are polycrystalline and exhibit twinning and considerable strain. These structures, however, are unstable, and annealing in the electron beam seems to cause the crystallites to revert to a single crystal morphology.

INTRODUCTION

The redispersion of supported metal catalysts by oxidation–reduction cycling has been of great interest to recent investigators (*1–11*), especially because of the drastic but reversible morphological changes of the metal crystallites observed during the cyclic treatment. Ruckenstein and Chu reported the redispersion of platinum on alumina after several cycles of alternate heating in O_2 and H_2 (*1*). They attributed the effect either to the spreading of platinum oxide over alumina or to the fracture of the crystallites. Subsequently, Ruckenstein and Chen (*2–4*) found that pits and cavities developed in Pd particles supported on alumina after O_2 treatment which disappeared upon reduction in H_2. The explanation proposed by the authors was that oxidation of Pd to PdO lowers its interfacial tension, causing it to spread on the unoxidized metal and leaving behind pits in the crystallite. Coalescence of pits gives rise to cavities. Similar morphological changes have been reported by Schmidt *et al.* working with Pt–Rh, Ir, and Rh supported on alumina and silica (*5–8*), Nishiyama *et al.* studying Ni crystallites dispersed on silica and alumina (*9, 10*) and Derouane *et al.* (*11*) studying Cu supported on MgO. Although these studies involved different metals, all of them have reported cavities or pits forming in the metal crystallites after the O_2 treatment, leading to a morphology often described as toroidal or horseshoe-shaped (*2–4, 9–11*).

Transmission electron microscopy (TEM) has been the major catalyst characterization technique in all of the above studies. The model catalysts studied were prepared by vacuum deposition of the metal onto planar oxide substrates having thicknesses less than 100 nm. A drawback in the use of these model catalysts is that information about the three-dimensional nature of the metal crystallites is obtained only in an indirect fashion (i.e., via weak beam microscopy or diffraction contrast). The metal crystallites are always imaged in projection through the oxide substrate.

---

[1] To whom correspondence should be addressed.

[2] Present address: Department of Metallurgy and Science of Materials, University of Oxford, Parks Rd., Oxford, OX1 3PH, England.

0021-9517/87 $3.00

Using the micrographs from the two-dimensional planar model catalysts one can only speculate but not make any definite conclusions about important factors affecting redispersion such as wetting of the support by the metal oxide, contact angles, and void formation between the oxide and the metal.

In this study, we report an alternative approach for studying the effect of oxidation–reduction treatment on Rh supported on silica. Our approach is based on the use of nonporous oxide particles of simple geometric shapes as catalyst supports (*12*). We have used silica spheres approximately 130 nm in diameter. These spheres are thermally stable in air and decrease negligibly in surface area at temperatures up to 1023 K. The spheres being nonporous, all the metal particles lie on the external surface and this enables imaging of the metal particles in projection as well as edge-on, thereby providing conclusive evidence about wetting and other surface phenomena mentioned above.

EXPERIMENTAL

The silica spheres were prepared by the aqueous hydrolysis of tetraethyl orthosilicate using NH_4OH as a buffer. The size of the spheres can be varied from 100 to 500 nm by changing the concentration of the reagents. The detailed preparation of the silica spheres has been described elsewhere (*13*). The catalyst was prepared with $Rh(acac)_3$ as the precursor by aqueous impregnation using 5 ml of water per gram of silica spheres. After impregnation, the catalyst was dried for 10 hr at 383 K and then reduced in flowing H_2 at 773 K overnight. This catalyst was coded RHS01a. Catalyst RHS01a was oxidized in 100 Torr O_2 at 823 K for 10 hr to get RHS01b (1 Torr = 133.3 Pa). The oxidized catalyst was subsequently reduced in 200 Torr H_2 at 473 K for 10 hr to obtain RHS01c. All catalyst samples were supported on holey carbon film for TEM studies. Electron microscopy was performed using a JEOL 2000-FX STEM at the University of New Mexico and a JEOL 4000-EX at Arizona State University. The point resolution in these microscopes is 0.3 nm and 0.17 nm, respectively. Chemisorption measurements were carried out in a static volumetric apparatus in which H_2 adsorption isotherms were recorded at 298 K and H_2 pressure of 0–160 Torr.

RESULTS AND DISCUSSION

Figure 1 shows a micrograph of RHS01a. Numerous small Rh crystallites are visible on the surface of the silica spheres, some of which lie at the edge of the spheres (arrowed), and can be seen edge-on. The contact angle between the metal particle and the support indicates that the crystallites do not wet the support. The particle size distribution is quite narrow with the average particle diameter being about 4.8 nm. Figure 2 shows a micrograph of RHS01c. All the crystallites now show characteristic areas of light contrast at the center. These micrographs are reminiscent of the toroidal morphology reported by earlier workers (*2–4, 9–11*). However, Fig. 2 shows that the crystallites look very similar when viewed in projection as well as edge-on. This indicates that the Rh particles are not toroidal or doughnut shaped, but appear to be equiaxed with a void or a cavity at the center. The areas of light contrast at the center look quite spherical despite the Rh crystallites themselves having fairly irregular shapes.

In order to understand the structure of these metal particles, the samples were examined in a high-resolution microscope operated at 400 keV where the lattice structure of the metal can be resolved. Figure 3 shows a micrograph of the catalyst RHS01a. The lattice fringes in this micrograph are consistent with fcc Rh. Figure 4 shows a micrograph of the Rh/SiO_2 catalyst after oxidation–reduction treatment (RHS01c). The characteristic areas of light contrast seen in the micrographs taken at 200 keV are again visible in these higher-resolution micrographs obtained at 400

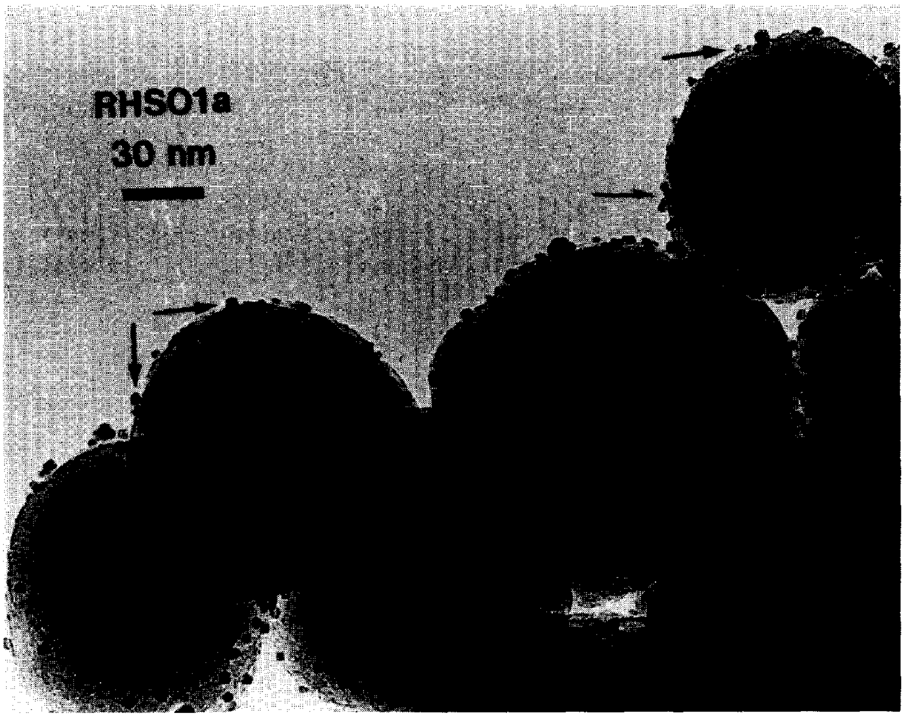

FIG. 1. Electron micrograph of catalyst RHS01a: 2 wt% Rh supported on 130-nm silica spheres.

FIG. 2. Micrograph of catalyst RHS01c obtained after oxidation of RHS01a at 823 K and subsequent reduction at 473 K.

FIG. 3. High-resolution electron micrograph of catalyst RHS01a.

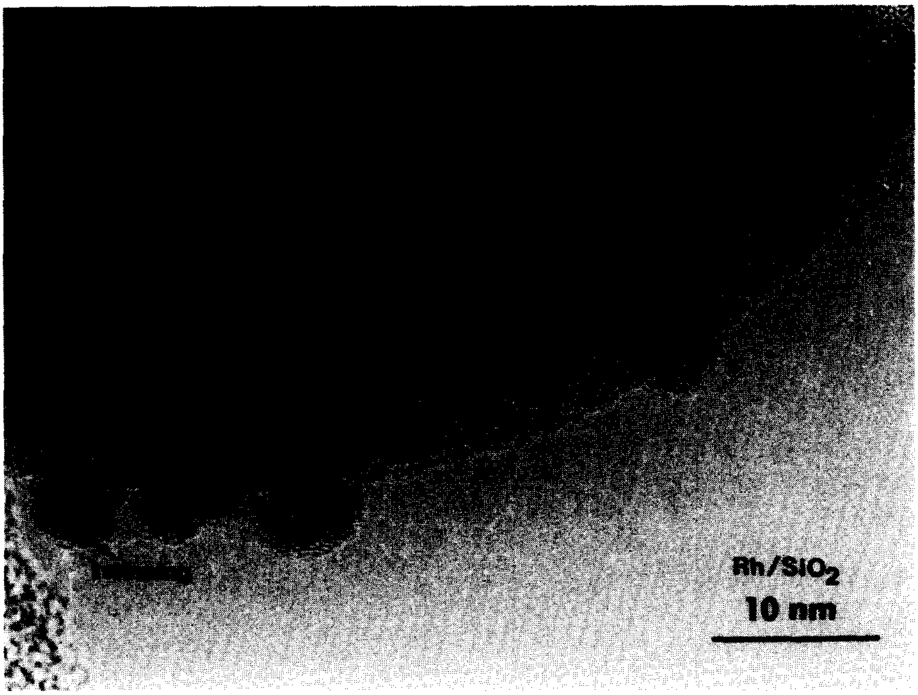

FIG. 4. High-resolution electron micrograph of catalyst RHS01c (obtained by oxidation-reduction treatment of RHS01a).

keV. Some of the metal crystallites are twinned and others appear polycrystalline with grain boundaries. Figure 5 shows a Rh crystallite where the lattice fringes are well resolved. The fringes in the periphery are those for Rh metal with different parts of the particle exhibiting different zone axes. However, the finer fringes in the core do not match those for Rh metal. Prolonged examination in the electron microscope seemed to anneal the particle, with the crystallite reverting to a single crystal morphology. The particle is poorly crystallized and appears to be under strain due to the mismatch between its subunits, and hence it reverts to a single crystal morphology because of the beam-induced heating.

Wang and Schmidt (*7*) found that Rh_2O_3 particles that were reduced at 423 K either split up into individual 1–2-nm crystallites or developed cracks within the particles. The reduction temperature was 473 K in this study and therefore it is possible that similar cracks may get partially annealed, leading to the polycrystalline Rh metal crystallites seen in Figs. 4 and 5. Thus, the results reported here are consistent with those of Wang and Schmidt (*7*). These authors also pointed out another mechanism for the formation of voids in a metal crystallite. When oxidation occurs at the outer surface of the particle, metal cations must diffuse through the oxide skin in order to get oxidized at the surface. On flat surfaces, the oxide skin can restructure by plastic flow (or split up and crack) in order for the oxidation to continue. However, on curved surfaces, restructuring of the oxide proves more difficult, and the process ultimately creates a void between the metal and the oxide. Oxidation ceases when such a void is formed, and the existence of such voids has been demonstrated in cross-sectional micrographs of Fe wires and at the corners of Fe cubes (*14*). Wang and Schmidt (*7*) postulated that complete oxida-

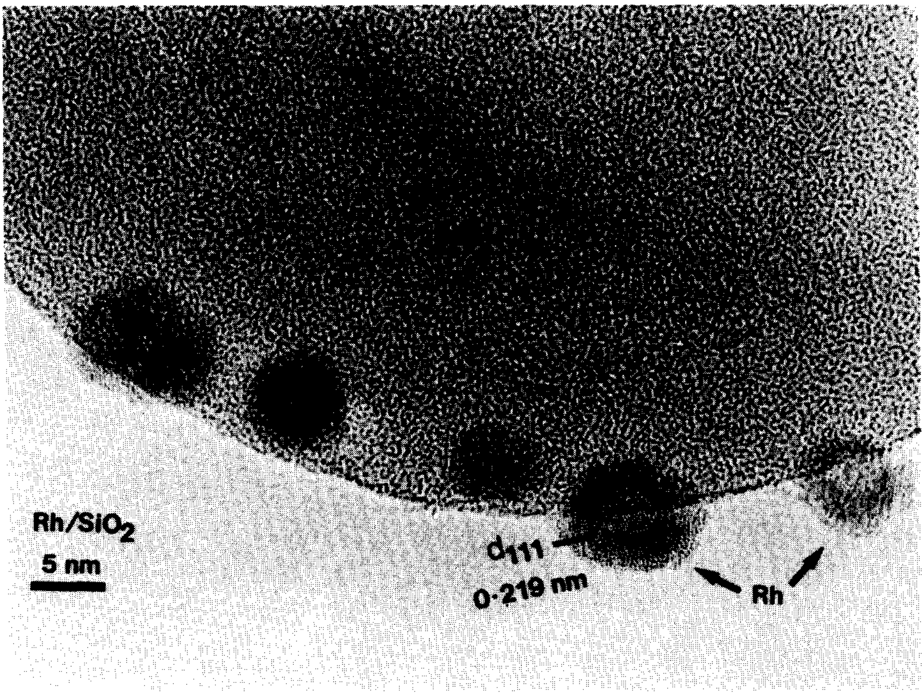

FIG. 5. High-resolution electron micrograph of catalyst RHS01c showing the unusual fringe contrast in the core of one of the crystallites.

tion of small metal particles could occur, despite the curved surfaces, when an alternative path exists for the cations to diffuse outward, i.e., along the interface between the particle and the oxide support. In such an event, the crystallite would spread along the support surface and develop a toroidal morphology. This does not seem to occur in the experiments reported here. Instead, the metal crystallites appear to oxidize uniformly without forming a void at the center. Figure 6 shows a micrograph of the oxidized catalyst RHS01b. The lattice spacings and interplanar angles are consistent with Rh_2O_3, and the doubling of the lattice fringes for the basal planes is typical of hexagonal crystal structures, suggesting that the oxide is hexagonal Rh_2O_3. None of the oxidized Rh particles shows evidence of voids or pits.

Comparison of Figs. 6 and 3 shows that the contact angle between Rh_2O_3 and SiO_2 is lower than that between Rh and SiO_2. The lower surface free energy of the oxide leads to a transition from nonwetting to wetting behavior. However, despite the change in contact angle, there is no significant spreading of the Rh_2O_3 on the silica. If we assume that there is no crystallite migration and coalescence, the volume of the oxide particle would be 1.91 times that of the metal crystallite (Rh: M.W. 102.9, ρ 12.424 and $RhO_{1.5}$: M.W. 126.9, ρ 8.02). For spherical particles, this would translate to a surface area increase of 54%. If the oxide particle retained its external shape during reduction, the resulting metal crystallite would exhibit an increase in chemisorption uptake of 54%. The chemisorption uptake of H_2 on catalyst RHS01a is 9.3 μmol/g and that on RHS01c is 12.13 μmol/g, an increase of 30%. The increase in surface area is less than that which would be predicted if the metal particle retained the external shape of the oxide particle from which it was formed. It appears that the oxide parti-

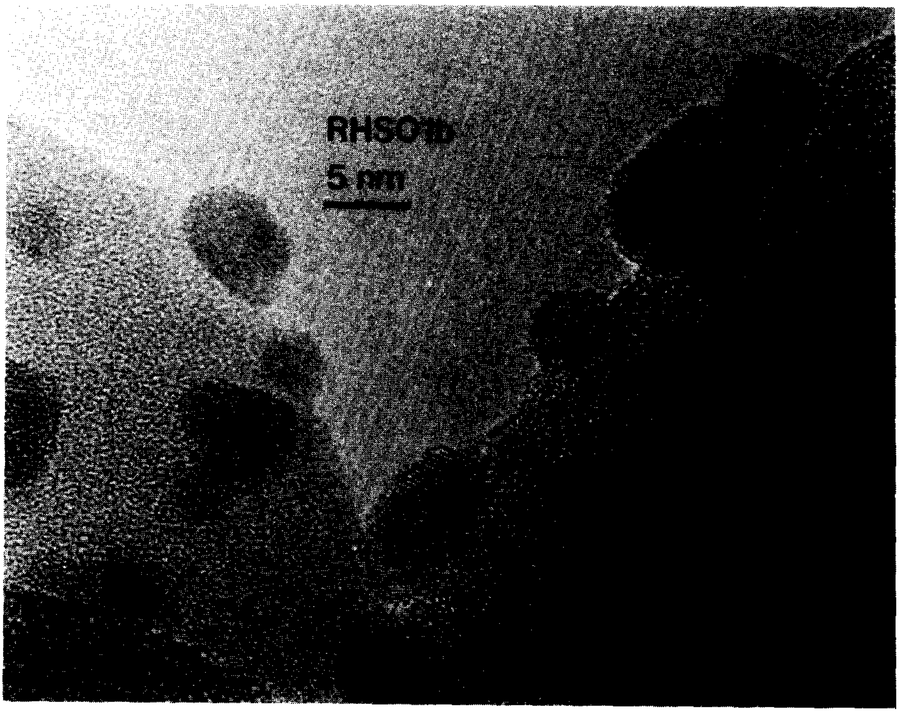

FIG. 6. High-resolution electron micrograph of catalyst RHS01b (obtained after oxidation of catalyst RHS01a).

cle contracts during reduction, but under the mild reduction conditions the metal is not mobile enough to restructure into a single crystal. Higher-temperature reduction would be expected to facilitate such a transformation, and the work of Lee and Schmidt (*8*) shows that the increased surface area observed after oxidation–reduction cycling is lost upon reduction at temperatures in excess of 473 K. In recent work on Ni/SiO_2, Lee *et al.* (*15*) found an increase in surface area of 40% after oxidation and subsequent reduction at 573 K, suggesting that a similar mechanism may be responsible for the surface area increase.

CONCLUSIONS

Nonporous silica spheres have been demonstrated to be excellent substrates for study of the three-dimensional structure of small metal crystallites. Since the metal crystallites reside on the external surface of the oxide support, it is possible to image the metal crystallites edge-on. The advantage of an edge-on view is that there is no underlying oxide support, and hence the resolution of the TEM images is considerably improved. Furthermore, since the silica spheres are 130 nm in diameter, it is possible to look through the support and image the metal crystallites in projection, perpendicular to the oxide surface. The edge-on and projected images permit a better understanding of the three-dimensional shapes of small metal crystallites and metal–oxide interfacial parameters.

The oxidation–reduction of Rh supported on silica causes dramatic changes in the morphology of the metal crystallites. This is because the metal crystallites grow in size upon oxidation because of the increased mass and the lower density of the oxide phase. Reduction at 473 K causes transformation to the metal but leaves a void in the center due to the volume difference between the oxide and metal. The crystallites which were single crystals in the original catalyst become polycrystalline with grain boundaries and considerable surface roughness and strain. This morphology appears to be unstable and the crystallites revert to single crystal form after prolonged examination in a 400-keV electron beam in the microscope. None of the metal crystallites studied developed pits or cavities after oxidation, in contrast to the observations reported in previous work (*1–11*). The Rh metal crystallites in this study are about 5 nm in diameter, whereas those in the previous work were considerably larger. Furthermore, the previous studies utilized planar supports while the support surface was spherical in this work. The shape and texture of the oxide surface and the diameter of the metal crystallites may play a role in determining the structure of the metal crystallites on a supported metal catalyst. We are investigating this further using oxide particles of other geometric shapes, e.g., cubes.

ACKNOWLEDGMENTS

This work was supported by a grant from the Engineering Foundation and from Sandia National Laboratories. Electron microscopy was performed at the Electron Microbeam Analysis Facility in the Department of Geology and the Institute of Meteoritics at the University of New Mexico. High-resolution microscopy was performed at the National Facility for High-Resolution Electron Microscopy, Arizona State University, supported by National Science Foundation grant DMR 83-06501.

REFERENCES

1. Ruckenstein, E., and Chu, Y. F., *J. Catal.* **59,** 109 (1979).
2. Ruckenstein, E., and Chen, J. J., *J. Catal.*, **70,** 233 (1981).
3. Chen, J. J., and Ruckenstein, E., *J. Phys. Chem.* **85,** 1606 (1981).
4. Ruckenstein, E., and Chen, J. J., *J. Colloid Interface Sci.* **86,** 1 (1982).
5. Chen, M., Wang, T., and Schmidt, L. D., *J. Catal.* **60,** 356 (1979).
6. Want, T., and Schmidt, L. D., *J. Catal.* **66,** 301 (1980).
7. Wang, T., and Schmidt, L. D., *J. Catal.* **70,** 187 (1981).
8. Lee, C., and Schmidt, L. D., *J. Catal.* **101,** 123 (1986).

9. Nakayama, T., Arai, M., and Nishiyama, Y., *J. Catal.* **79,** 497 (1983).

10. Nakayama, T., Arai, M., and Nishiyama, Y., *J. Catal.* **87,** 108 (1984).

11. Derouane, E. G., Chludzinski, J. J., and Baker, R. T. K., *J. Catal.* **85,** 187 (1984).

12. Datye, A. K., and Logan, A. D., *Proc. 44th Meet. Electron Microsc. Soc. Amer.* (G. W. Bailey, Ed)., p. 772, (1986).

13. Huizenga, D. G., and Smith, D. M., *AIChE J.* **32,** 1 (1986).

14. Engell, H. J., and Weaver, F., *Acta Metallurg.* **5,** 695 (1957).

15. Lee, C., Schmidt, L. D., Moulder, J. F., and Rusch, T. W., *J. Catal.* **99,** 472 (1986).